

9-7-1991

## The Measurement of Aluminum Surface Diffusion on Si, SiO<sub>2</sub>, and Si<sub>3</sub>N<sub>4</sub> by Scanning Auger Microscopy

L. L. Levenson

*University of Colorado, Colorado Springs*

A. B. Swartzlander

*Solar Energy Research Institute*

A. Yahashi

*Kyoto University*

H. Usui

*Kyoto University*

I. Yamada

*Kyoto University*

Follow this and additional works at: <https://digitalcommons.usu.edu/microscopy>

 Part of the [Biology Commons](#)

---

### Recommended Citation

Levenson, L. L.; Swartzlander, A. B.; Yahashi, A.; Usui, H.; and Yamada, I. (1991) "The Measurement of Aluminum Surface Diffusion on Si, SiO<sub>2</sub>, and Si<sub>3</sub>N<sub>4</sub> by Scanning Auger Microscopy," *Scanning Microscopy*: Vol. 5 : No. 3 , Article 10.

Available at: <https://digitalcommons.usu.edu/microscopy/vol5/iss3/10>

This Article is brought to you for free and open access by the Western Dairy Center at DigitalCommons@USU. It has been accepted for inclusion in Scanning Microscopy by an authorized administrator of DigitalCommons@USU. For more information, please contact [digitalcommons@usu.edu](mailto:digitalcommons@usu.edu).



## THE MEASUREMENT OF ALUMINUM SURFACE DIFFUSION ON Si, SiO<sub>2</sub>, AND Si<sub>3</sub>N<sub>4</sub> BY SCANNING AUGER MICROSCOPY

L.L. Levenson<sup>1\*</sup>, A.B. Swartzlander<sup>2</sup>, A. Yahashi<sup>3</sup>, H. Usui<sup>3</sup>, and I. Yamada<sup>3</sup>

<sup>1</sup>Department of Physics and Energy Science, University of Colorado, Colorado Springs,  
CO 80933-7150, <sup>2</sup>Solar Energy Research Institute, 1617 Cole Boulevard, Golden, CO 80410,

<sup>3</sup>Ion Beam Engineering Experimental Laboratory, Kyoto University, Kyoto 606, Japan

(Received for publication August 25, 1990, and in revised form September 7, 1991)

### Abstract

The diffusion distance of Al atoms on Si(111), SiO<sub>2</sub>, and Si<sub>3</sub>N<sub>4</sub> substrates has been measured as a function of substrate temperature. These studies were carried out by depositing Al from an effusive source and from an ionized cluster beam source. Both sources were used in the same apparatus at different times. The deposition was carried out with either a slit mask or a wire mask at the substrate. After the masks were removed, the deposit was examined by optical and electron microscopy, mechanical profilometer, and Auger line scans. The diffusion distance of Al on the substrates was determined from these measurements. The largest diffusion distances measured on all surfaces occurred at a substrate temperature of 200°C. The maximum diffusion distance at 200°C is due to a competition between increasing surface mobility and desorption of Al atoms as surface temperature increases.

**Key Words:** Aluminum, surface diffusion on Si(111), silicon oxide, silicon nitride, ionized cluster beam deposition, physical vapor deposition.

\*Address for correspondence:

Leonard L. Levenson, Department of Physics and Energy  
Science, University of Colorado, Colorado Springs, CO  
80401, Phone No. (719) 593-3283

### Introduction

The surface mobility of deposited atoms is dependent on several parameters, including substrate temperature, the bonding energy of deposited atoms to the substrate and to other surface atoms, and to surface structure. Localized surface mobility may be influenced by the kinetic energy of impinging atoms and ions. However, the thermalization of atoms on a surface is expected to be rapid. Therefore, surface diffusion is likely to be dominated by atoms in thermal equilibrium with the substrate.

Information about the surface mobility of Al atoms on various substrates is of interest because Al contacts and interconnections are widely used on Si based integrated circuits. In particular, it appears that high atom mobility during Al deposition results in improved step coverage at vias and contacts, and that high Al mobility also contributes to improved planarization.<sup>4</sup>

Recently, the surface mobility of Al on Si(111)<sup>5,6</sup> on silicon oxide<sup>7-9</sup> and on silicon nitride<sup>9</sup> has been determined for ionized cluster beam (ICB), neutral cluster deposition (NCD), and physical vapor deposition (PVD). In all these studies the deposit edges were defined by a shadow mask. During Al deposition on Si(111) substrates, a mask with 50 μm wide slits was held 0.1 mm below the substrate so that Al atoms arriving on the substrate were free to diffuse under the mask edge. For NCD and ICB deposition of Al on Si(111), the diffusion distance of Al was found to range from 10 to 40 μm. Furthermore, the diffusion distance was dependent on substrate temperature during NCD and ICB deposition and on acceleration voltage during ICB deposition.<sup>6</sup> Wire shadow masks were used to produce shadow zones on the surfaces of samples during NCD, ICB and PVD of Al on silicon oxide and silicon nitride substrates.<sup>7-9</sup> The Al diffusion distance ranged from 8 to 30 μm on silicon oxide substrates during NCD and ICB deposition.<sup>8</sup> The Al diffusion distance on silicon nitride ranged from 20 to 25 μm during PVD at various substrate temperatures.<sup>9</sup> For all substrates, the maximum diffusion distance of Al occurred at a substrate temperature near 200°C for every NCD, ICB and PVD condition. A brief description of the experimental parameters is given in the following section.

### Experimental

The Si(111) substrates were cut 4° off axis in the [110] direction. These substrates were cleaned by thermal

desorption of a weak oxide at 850°C for 15 min at the pressure of  $5 \times 10^{-10}$  Torr. Part of the substrate was covered by a 0.1-mm-thick stainless-steel mask. This mask was held 0.1 mm from the substrate by a Mo spacer. Slots 50  $\mu\text{m}$  wide  $\times$  1 mm in the mask allowed Al to be deposited on the substrate. The source of Al vapor was a graphite crucible in an ionized cluster beam (ICB) source. The ICB source was similar to the one described by Takagi.<sup>11</sup> The crucible nozzle was 2 mm in diameter and 2 mm in length. The crucible was operated at 1500°C and contained 99.999 wt. % pure Al. A shutter between the source and the substrate allowed the source conditions to be stabilized before deposition began. The deposition rate was 6 nm/min and the deposition time was 1 min. The nozzle-substrate distance was 225 mm.

For deposition on Si(111), the Al source was operated in two modes. In the neutral cluster deposition (NCD) mode, the cluster ionization section was turned off and no acceleration voltage was used. The ionized cluster beam (ICB) mode used a 200 V, 100 mA electron current to partially ionize the cluster beam, and a 3 kV voltage was used to accelerate the ionized portion of the Al beam. In-situ Auger electron spectroscopy of the surface after each deposition only showed the presence of Al and Si. No impurities could be detected on the surface. Ex-situ Auger line scans of the Al strips were carried out with a PHI model 600 SAM to measure the diffusion distance of Al atoms under the mask edge. The primary electron beam energy was 5 keV and the beam diameter used for the line scans was about 1  $\mu\text{m}$ .

The deposition of Al on various silicon oxide and silicon nitride substrates was carried out in a vacuum chamber held at  $2 \times 10^{-6}$  Torr by a liquid nitrogen trapped oil diffusion pump. An Al vapor source used graphite crucibles and was designed for ICB deposition. However, NCD and ICB deposition could be carried out with one crucible with a 2 mm diameter nozzle by using no ionization current or acceleration voltage in the former case. In the ICB mode an electron current at 200 mA, 400 V was used for ionization of the Al beam, and 3 kV and 6 kV voltages applied for acceleration of the ions.

For physical vapor deposition (PVD) of Al, a graphite crucible with a 5.5 mm diameter orifice was placed in the source. No other source parameters were changed. The large orifice on the crucible prevented any formation of clusters in the Al beam. All crucibles were filled with 99.999 wt. % purity Al and operated at 1500°C. The crucible to substrate distance was 240 mm.

The substrates consisted of Si coated with various silicon oxides and with silicon nitride. All coatings were between 0.5 and 1  $\mu\text{m}$  thick. The roughness average,  $R_a$ , of the samples was measured with a DEKTAK Model 3030 profilometer. The samples are described in Table 1. Before being mounted in the deposition chamber, each sample had two wire masks attached to it. The wire used was made of chromel (chromel-aluminum alloy) and it was nominally 50  $\mu\text{m}$  in diameter. Just before deposition of Al was started, the samples were heated to between 600°C and 800°C. Then the sample temperature was allowed to fall to the temperature chosen for the experiment. A shutter was used to start and stop the deposition. Immediately after the Al depositions, the samples were allowed to cool to room temperature. The wire shadow masks were removed from the samples and the shadow areas were examined by optical and scanning electron microscopy, mechanical profilometry, and Auger electron line scans.

## Results

It is known that vicinal Si(111) surfaces, misoriented toward the [110] direction, reconstruct into clusters of steps separated by (111) planes.<sup>10</sup> Since the Si(111) sample used for surface diffusion measurements of Al was off-cut in the [110] direction, the slots in the mask used for these measurements were oriented in different directions to determine if surface diffusion is anisotropic. The slots in the 90° mask were oriented perpendicular to the expected direction of step edges on the Si(111) substrate. Fig. 1 shows an Auger Al LVV line scan across an Al strip deposited through the 90° mask. Fig. 2 shows the same line scan recorded at higher resolution on an x-y plotter. These line scans show that significant surface diffusion takes place on the substrate under the mask edge during the deposition at a substrate temperature of 200°C.

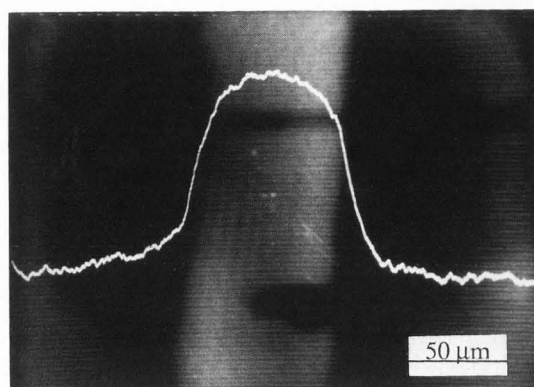


Figure 1. Aluminum LVV Auger line scan superimposed on scanning electron microscope image of an Al strip on Si(111) substrate. The Al was deposited through a slot oriented perpendicular to step edges on the 4° off-cut Si substrate. The film thickness was  $\sim 6$  nm. Substrate temperature during deposition was 200°C, and neutral cluster deposition of Al was used.

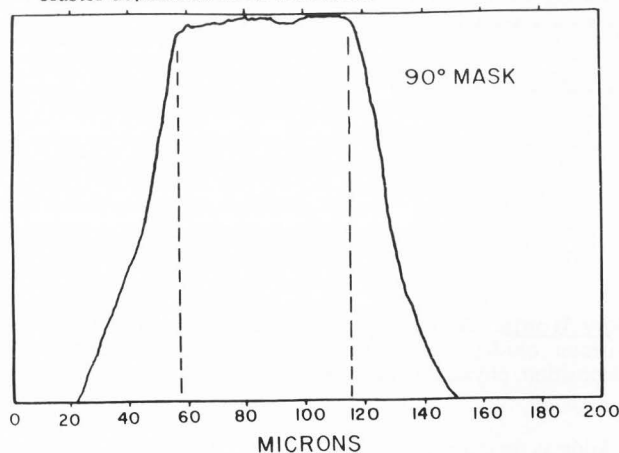


Figure 2. Detailed recording of the Al LVV Auger line scan shown in Fig. 1. The fall-off of the Auger signal is symmetric on both sides of the Al strip.

Fig. 3 is the Al Auger line scan of an Al strip deposited through a slot oriented parallel to the step edges, i.e., with a 0° orientation to step edges. This line scan is highly asymmetric. It indicates that surface diffusion is not equal on both sides of the slot, i.e., the surface mobility of Al is not the same in the [110] and  $\bar{1}\bar{1}0$  directions.

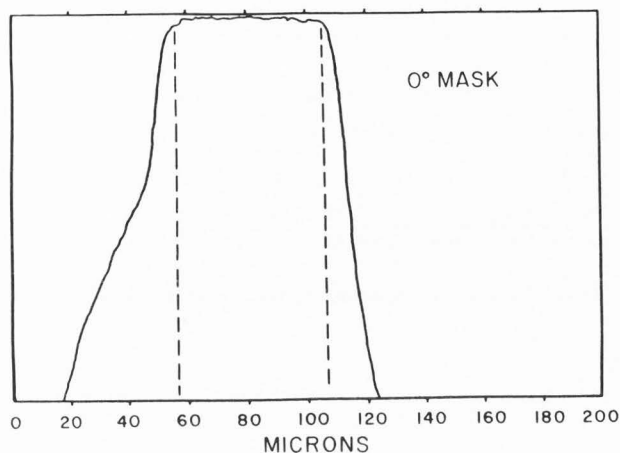


Figure 3. Al LVV Auger line scan of an Al strip deposited through a slot oriented in the directions of the steps on the Si surface. This Al strip was deposited at the same time and on the same substrate used for the data in Figs. 1 and 2.

The distance between the point where the Auger signal begins to roll off from the maximum (indicated by the vertical broken lines in Figs. 2 and 3) to the point of zero signal was taken as the diffusion distance under the mask edge. These distances were determined for the  $\bar{1}\bar{1}0$  and  $\bar{1}\bar{1}0$  directions. They are given in Table 2 as a function of acceleration voltage and surface temperature. The acceleration voltage of 0 kV indicates NCD, while 3 kV indicates ICB deposition. The results of Table 2 are plotted in Fig. 4. Note that in all cases, the maximum diffusion distance occurs at a substrate temperature near 200°C.

Fig. 5 is the recording of an Auger line scan across the shadow zone produced by the presence of a wire mask on the NCR high temperature oxide during NCD of Al. A profilometer trace of the same shadow zone showed the Al film thickness to be about 150 nm and the shadow zone to be 56  $\mu\text{m}$  wide at the top. The top of the Auger line scan in Fig. 5 is also 56 nm wide. The roll-off of the Auger signal on each side of the shadow zone is due to the diffusion of Al under the edge of the wire mask. The diffusion distances on each side of the shadow are symmetric, as one would expect on an amorphous surface. The rapid fall-off of the Auger signal shows that the diffusion of Al into the shadow zone forms a film much thinner than the Al film outside the shadow zone. The diffusion distance is taken from the edge of the Auger signal maximum (shadow zone outer edge) to the point where the Auger signal first reaches zero. These diffusion distances for NCD (0 kV) and ICB (3 and 6 kV) deposition onto the NCR HTO and LTO silicon oxide substrates are shown in Table 3 and in Fig. 6. Again, it is seen that the maximum diffusion distance occurs for substrate temperatures near 200°C.

Physical vapor deposition (PVD) of Al with the 5.5 mm diameter orifice on the graphite crucible was also done

with wire shadow masks placed on the substrate described in Table 1. The Auger line scans yielded the diffusion distances shown in Table 4 and Fig. 7. In Fig. 7, the data from Table 3 for neutral cluster deposition (NCD) of Al are included for the sake of comparison. It is apparent that the maximum diffusion distance near 200°C holds for this data.

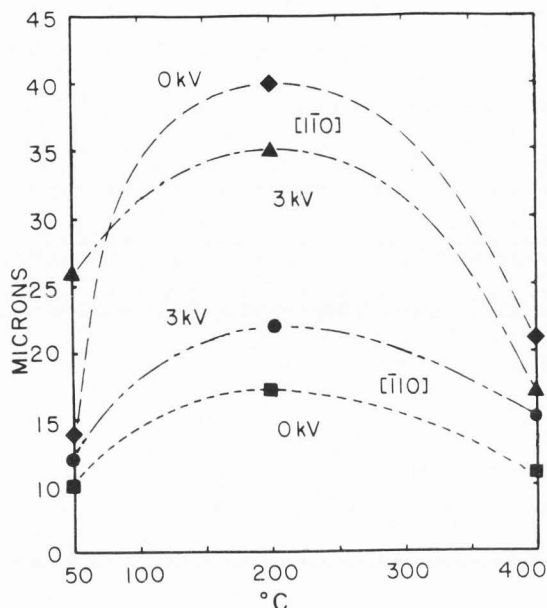


Figure 4. Graph of the results given in Table 2. The dependence of Al diffusion distance on the diffusion direction is indicated. The solid diamonds are for 0 kV and the solid triangles are for 3 kV acceleration in the  $\bar{1}\bar{1}0$  direction, while the solid squares are for 0 kV and the solid circles are for 3 kV acceleration in the  $\bar{1}\bar{1}0$  direction respectively.

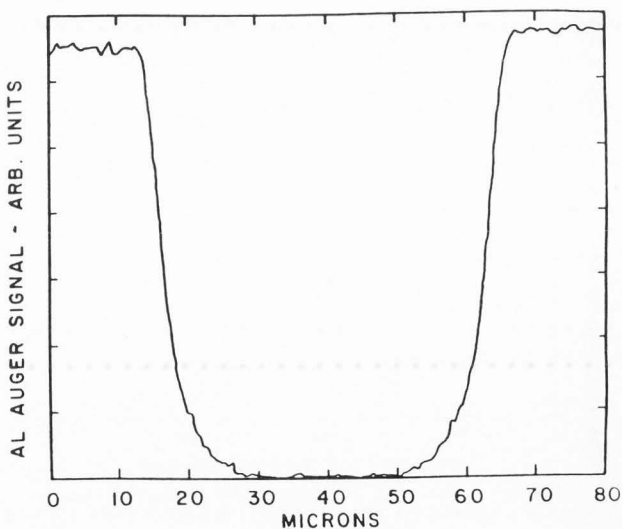


Figure 5. Auger line scan of the shadow zone after neutral cluster beam deposition of Al on NCR HTO at substrate temperature of 80°C.

Table 1. Description of Samples

Sample Name	Preparation	Surface Roughness
NCR HTO	Steam oxidation of Si at 900°C	R <sub>a</sub> = 0.4 nm
NCR HTO	P-doped plasma CVD SiO <sub>2</sub> at 425°C	R <sub>a</sub> = 0.8 nm
Minolta HTO	Oxidation of Si at 1100°C	R <sub>a</sub> = 0.5 nm
Novellus LTO	Plasma CVD SiO <sub>2</sub> at 400°C	R <sub>a</sub> = 1.6 nm
Novellus Nitride	Plasma CVD Si <sub>3</sub> N <sub>4</sub> at 400°C	R <sub>a</sub> = 3.6 nm

Table 2. Diffusion distance of Al on Si(111) cut 4° off axis as a function of acceleration voltage, substrate temperature, and diffusion direction.

Acceleration voltage (kV)	Surface temperature (°C)	Diffusion distance (μm)	
		[110]	[110]
0	50	10	14
3	200	12	26
0	200	17	40
3	200	22	35
0	400	11	21
3	400	15	17

Table 3. Aluminum diffusion distance at HTO and LTO SiO<sub>2</sub> during ionized cluster beam deposition.

Acceleration voltage (kV)	Substrate temperature (°C)	Diffusion distance (μm)	
		on HTO (μm)	on LTO (μm)
0	80	15	8
3	70	22	8
6	80	26	11
0	200	26	11
3	200	25	14
6	200	29	19
0	400	24	12
3	400	19	10
6	400	12	10

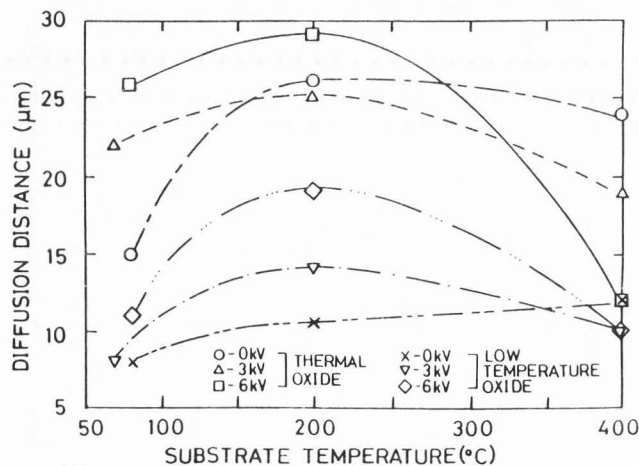


Figure 6. Diffusion distance of Al for neutral cluster beam deposition (0 kV) and ICB deposition (3 and 6 kV) on NCR HTO thermal (thermal oxide) and LTO silicon oxide substrates.

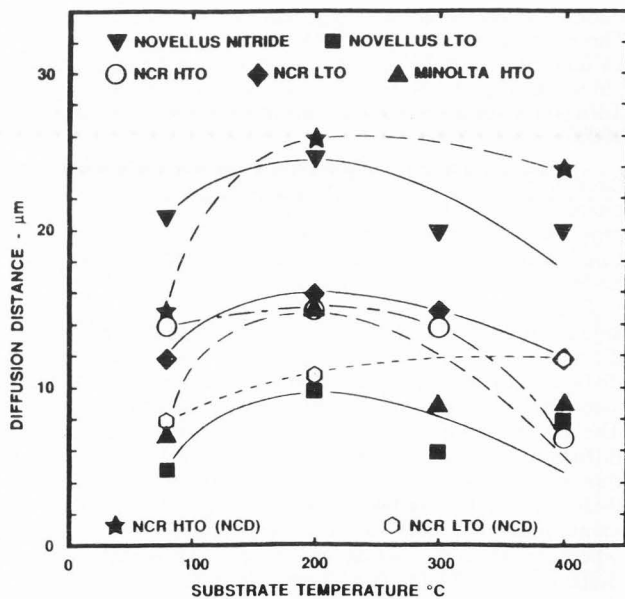


Figure 7. Diffusion distance of Al on various substrates as a function of substrate temperature during physical vapor and neutral cluster deposition.



Table 4. Al Diffusion distance ( $\mu\text{m}$ ) as a function of substrate temperature for various silicon oxides and silicon nitride.

Temperature	NCR HTO		NCR LTO		MINOLTA LTO	NOVELLUS LTO	NOVELLUS NITRIDE
	NCD*	PVD#	NCD	PVD	PVD	PVD	PVD
80	15	14	8	12	7	5	21
200	26	15	11	16	15	10	25
300	--	14	--	15	9	6	20
400	24	7	10	12	9	8	20

### Discussion

The Al diffusion distance data show two distinct features. The first is the maximum which appears near 200°C independent of substrate composition and surface roughness. Venables et al. have found similar maxima from their diffusion distance measurements of Ag on Si(111) substrates.<sup>13</sup> This behavior can be explained in terms of surface diffusion, nucleation and desorption of Ag atoms. At low temperatures, desorption is almost non-existent while the nucleation of atoms into clusters is rapid. Therefore, at low temperatures, the effective surface mobility is reduced by the capture of diffusing atoms by nuclei. As temperature increases, nucleation processes are reduced and surface diffusion distances increase. However, thermal desorption increases exponentially with increasing temperature. At a certain temperature the increase in surface mobility is offset by the increase in thermal desorption. At that temperature, the effective diffusion distance begins to decrease. This model<sup>13</sup> also fits our observations for Al surface diffusion as a function of temperature for all substrates tested.

The second prominent feature of our data is the magnitude of the measured diffusion distances, i.e., displacements of tens of micrometers. Such large displacements are most likely the result of thermal diffusion rather than the outcome of dynamic surface scattering of atoms or the breakup of clusters. In the case of atoms, Dodson<sup>2</sup> has made an atomic simulation of the impact of Si atoms on Si(111) substrates. Even with kinetic energies of 10 eV and a perpendicular incidence at the surface, Si atoms are expected to be captured with a probability of unity and to come to rest within a few atomic distances of the point of impact. As for cluster-surface impact, a computer simulation by Yamamura and Yamada<sup>14</sup> shows that the breakup of ionized Ag clusters on an amorphous carbon surface should produce a spread of Ag atoms to distances below 50 nm from the collision center. In this computer model, the average kinetic energy of the Ag clusters before impact was 5 eV/atom. The results of these computer simulations indicate that Al surface diffusion displacements of tens of  $\mu\text{m}$  are unlikely to be caused by dynamic surface scattering of Al atoms. Therefore, it is appropriate to analyze the data accumulated here on the basis of equilibrium surface diffusion. Only a few simple assumptions are required for this analysis.

The first assumption is that the edge of the masked area defines the starting point for diffusion into the shadowed area. Atoms impacting at this edge will have the highest probability of diffusing to the maximum displacement into the shadowed area. Let X be the mean surface displacement from the point of impact. X can be expressed as<sup>1</sup>

$$X = (2D_s \tau_s)^{1/2} \quad (1)$$

where  $D_s$  is the surface diffusion coefficient and  $\tau_s$  is the mean time interval between impact and desorption from the surface.  $D_s$  and  $\tau_s$  are both temperature dependent as shown by the following equations:<sup>1</sup>

$$D_s = a^2 \nu \exp(-Q_{\text{diff}}/kT) \quad (2)$$

$$\tau_s = (1/\nu) \exp(Q_{\text{des}}/kT) \quad (3)$$

where  $a$  and  $\nu$  are the jump distance and frequency, and  $Q_{\text{diff}}$  and  $Q_{\text{des}}$  are the energies required for diffusion and desorption. Substituting Eqs. 2 and 3 into Eq. 1 gives

$$X = (2)^{1/2} a \exp[(Q_{\text{des}} - Q_{\text{diff}})/kT] \quad (4)$$

Let  $(Q_{\text{des}} - Q_{\text{diff}}) = \Delta Q$ . Then,

$$X = (2)^{1/2} a \exp(\Delta Q/2kT) \quad (5)$$

Next, assume  $X=x/2$ , where  $x$  is the maximum diffusion distance measured for Al. Then, assuming  $a=0.3$  nm to be the jump distance of Al atoms from one absorption site to another,  $\Delta Q$  can be expressed in terms of the absolute substrate temperature  $T$  and  $x$ :

$$\Delta Q = 1.72 \times 10^{-4} T \ln(1.18 \times 10^9 x) \quad (6)$$

where  $x$  is given in meters and  $\Delta Q$  is in eV/atom. The values of  $\Delta Q$  obtained from the diffusion distances  $x$  in Tables 2, 3 and 4 are shown in Tables 5, 6 and 7. It is apparent that  $\Delta Q$  increases with substrate temperature, and for a given substrate temperature,  $\Delta Q$  does not vary greatly with the substrate composition. Furthermore,  $\Delta Q$  does not appear to be very sensitive to variations in surface roughness among the different substrates. The spread in  $\Delta Q$  from 0.52 to 1.19 eV/atom seems reasonable compared to  $Q_{\text{des}}=0.9$  eV found for Al on mica.<sup>1</sup> It should be recalled that  $Q_{\text{diff}}$  is usually only a fraction of the value of  $Q_{\text{des}}$ .<sup>1</sup>

As for the variation of  $\Delta Q$  with temperature, it is well to recall that even for gas phase and liquid phase reactions the "activation energy" is often temperature dependent. For example, this is the case for the classic studies of the rate of catalyzed hydrolysis of sucrose and the gaseous reaction  $\text{H}_2 + \text{I}_2 \rightarrow 2\text{HI}$ .<sup>3</sup> For this study, it is of interest to note that  $\ln \Delta Q$  vs temperature is a linear function of  $1/T$ . This is illustrated in given in Tables 5, 6 and 7. These results can be expressed in the form,

$$\Delta Q = \Delta Q_0 \exp(-E/kT) \quad (7)$$

where  $E$  is an energy term (eV/atom) and  $\Delta Q_0$  is the pre-exponential value given for the temperature  $T$  at which  $\Delta Q=1.0$  eV/atom ( $\ln \Delta Q=0$ ). In Eq.7,  $-E/k$  is the slope of the line in Figs. 8-10. Values of  $\Delta Q_0$  and  $E/k$  are given in Table 8.

The combination of Eqs. 5 and 7 and the assumption that  $X=x/2$  give

$$x = (2)^{3/2} a \exp [(\Delta Q_0/2kT) \exp (-E/kT)] \quad (8)$$

In Eq. 8, the only adjustable parameter is the atom jump distance  $a$ . The experimental parameters are  $x$  and  $T$ , which are measured, and  $\Delta Q_0$  and  $E/k$  which are determined from the values of  $\Delta Q$  vs  $T$ . Now, the determined values of  $\Delta Q_0$  and  $E/k$  in Table 8 and an assumed value for the jump distance  $a=0.3$  nm can be used to calculate the diffusion distance  $x$  as a function of  $T$  during Al deposition on the various substrates from ICB and PVD sources. The result of this calculation is shown in Fig. 11. It can be seen that the calculated behavior of diffusion distance  $x$  vs  $T$  mimics the measured diffusion distances found from Auger line scans. There is a maximum diffusion distance near a substrate temperature of 200°C in all cases. The combined results of physical vapor deposition produce diffusion distances that tend to be smaller than diffusion distances produced by ICB sources for both neutral and ionized beam conditions.

Although Eq. 8 allows the experimental results to be mimicked, the physical meaning of  $\Delta Q_0$  and  $E$  is not transparent. Also, it is not satisfactory to have varying values of  $\Delta Q$ , since one ordinarily seeks constant  $Q_{des}$  and  $Q_{diff}$ . One reason that  $\Delta Q$  varies as it does with  $T$  is probably related to the details of the nucleation processes and the formation of Al clusters or islands on the substrates under the mask edges during Al deposition.

In these experiments, the population density and size distribution of Al islands varied as a function of time and distance from the mask edge. The variation in population density and island size on Si(111) with distance from the mask edge is illustrated in Figs. 12 and 13. In Fig. 12a and Fig. 12b, the Al islands are seen to decrease

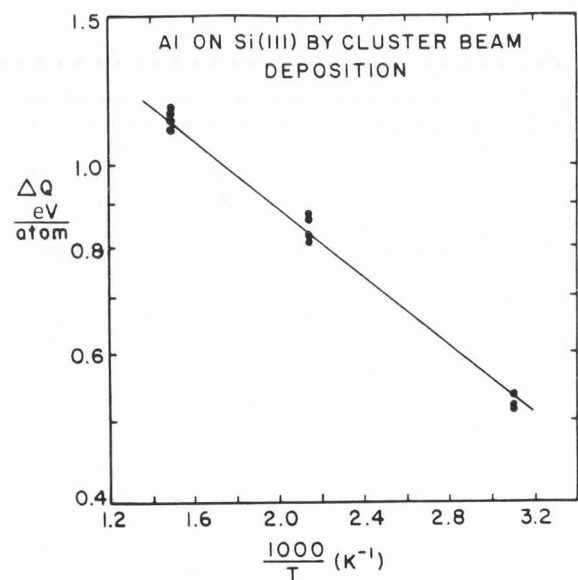


Figure 8. Semi-log plot of all values of  $\Delta Q$  vs  $1000/T$  from Table 5, where  $T$  is the absolute substrate temperature.

in size as the distance from the mask edge, shown beneath the micrographs, increases. In this case, the nominal Al film thickness was only 6 nm and the substrate temperature was 400°C. The film in Fig. 12a was produced by a partially ionized beam and an acceleration voltage of 3 kV, while the film in Fig. 12b was not ionized and had no acceleration voltage.<sup>5,6</sup> In both cases, the deposition time was 1 min. Fig. 13 shows various micrographs of an Al film at the edge of the shadow zone produced by a wire mask. The film was deposited by PVD of Al onto NCR

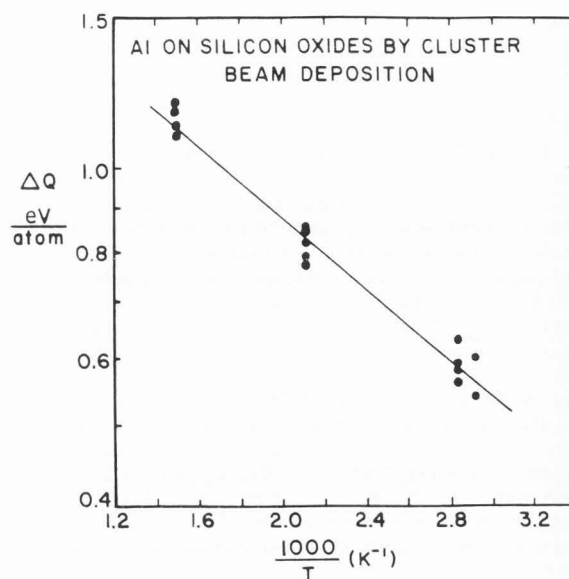


Figure 9. Semi-log plot of all values of  $\Delta Q$  vs  $1000/T$  from Table 6, where  $T$  is the absolute substrate temperature.

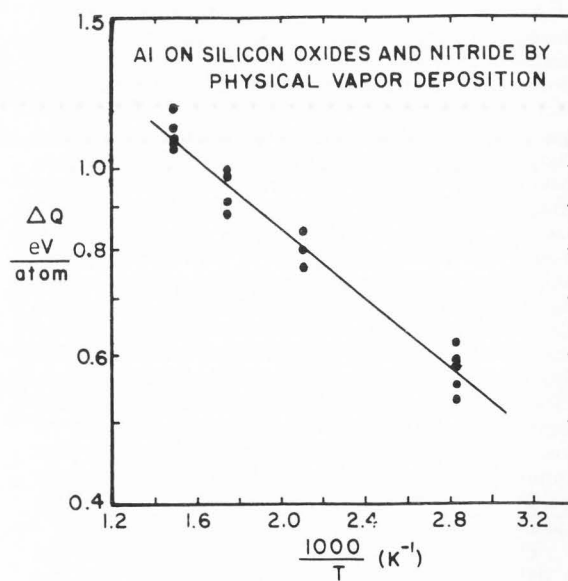


Figure 10. Semi-log plot of all values of  $\Delta Q$  vs  $1000/T$  from Table 7, where  $T$  is the absolute substrate temperature.

Table 5. ΔQ (eV/atom) as a function of substrate temperature, diffusion direction, and acceleration voltage for ICB deposition of Al on 4° off cut Si(111).

Substrate Temperature (°C)	Diffusion Direction and Acceleration Voltage			
	[110] 0 kV	[110] 3 kV	[110] 0 kV	[110] 3 kV
50	0.52	0.53	0.54	0.57
200	0.81	0.83	0.88	0.86
400	1.10	1.13	1.17	1.15

Table 6. ΔQ (eV/atom) as a function of substrate temperature and acceleration voltage for ionized cluster beam deposition of Al on HTO and LTO SiO<sub>2</sub>.

Acceleration voltage (eV)	Substrate temperature (°C)	ΔQ for HTO (eV/atom)	ΔQ for LTO (eV/atom)
0	80	0.59	0.56
3	70	0.60	0.54
6	80	0.63	0.58
0	200	0.84	0.77
3	200	0.84	0.79
6	200	0.85	0.82
0	400	1.19	1.11
3	400	1.16	1.09
6	400	1.11	1.09

high temperature oxide (Table 1 at a substrate temperature of 300°C. In this case the film thickness was 270 nm and the deposition time was 15 min. The left hand micrograph in Fig. 13 shows the shadow zone at low magnification. The upper row of photos images the left edge of the shadow zone and the lower row shows the right edge. The magnification increases from left to right. At 60k magnification, it is clear that Al island size decreases sharply as distance from the edge of the shadow zone increases. Given the variation of experimental conditions and substrates, it is interesting that the experimental results and the parameters of Table 8 applied to Eq. 8 show similar curves in Fig. 11 for Al diffusion distance under a mask edge versus substrate temperature.

Table 7. ΔQ (eV/atom) as a function of substrate temperature.

Temperature °C	NCR HTO		NCR LTO		MINOLTA HTO	NOVELLUS LTO	NOVELLUS NITRIDE
	NCD*	PVD#	NCD	PVD	PVD	PVD	PVD
80	0.59	0.59	0.56	0.58	0.55	0.53	0.62
200	0.84	0.80	0.77	0.80	0.80	0.76	0.84
300	---	0.97	---	0.96	0.91	0.88	0.99
400	1.19	1.05	1.09	1.11	1.08	1.06	1.17

\*NCD = neutral cluster deposition

#PVD = physical vapor deposition

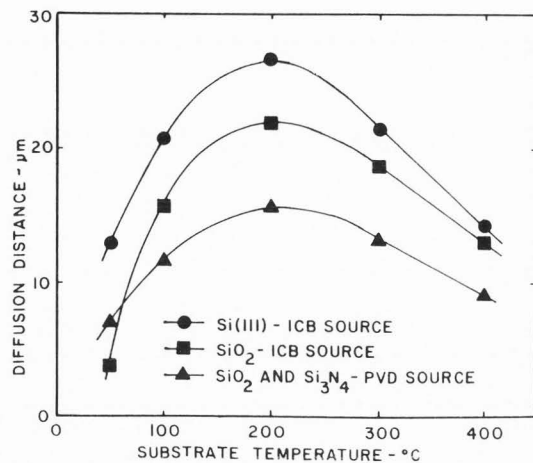


Figure 11. Diffusion distance calculated from Eq. 8 using values of ΔQ<sub>0</sub> and E/k in Table 8 and assuming an Al atom jump distance a=0.3 nm.

Table 8. Linear regression values of ΔQ<sub>0</sub> and E/k calculated from Tables 5-7.

Al from	Table number	ΔQ <sub>0</sub> eV/atom	E/k K
ICB source onto Si(111)	5	2.24	462
ICB source onto SiO <sub>2</sub>	6	2.27	478
PVD source onto SiO <sub>2</sub> and Si <sub>3</sub> N <sub>4</sub>	7	2.17	473

The experimental method used here does not permit us to take advantage of the theoretical techniques developed by Venables et al.<sup>12,13</sup> to estimate various bonding energies. The methods of Venables and those of Zinke-Allmang and Feldman<sup>15</sup> to determine the activation energy and pre-exponential factor for surface diffusion give better insight into the physics of surface processes than the method used here. However, we have shown that Al surface diffusion under a mask edge during deposition shows similar characteristics over a wide range of experimental conditions. Also, we have developed an empirical relationship (Eq. 8) which depends only on one selectable parameter (atom jump distance) and two



Fig. 12a.

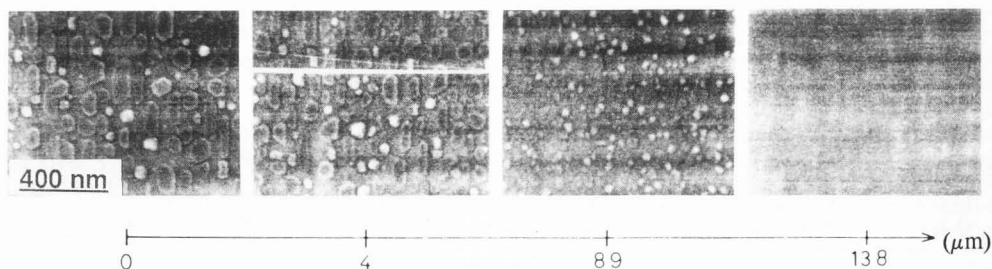


Fig. 12b.

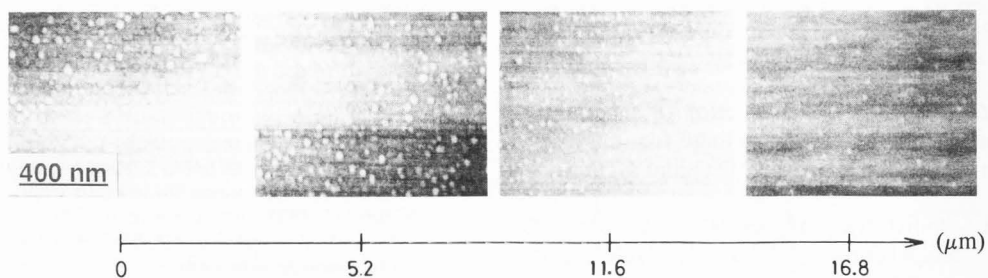


Figure 12. Scanning electron micrographs of Al platelets and islands at various distances from the mask edge in the [110] direction on Si (111). Nominal film thickness is 6 nm. Substrate temperature: 400°C. Acceleration voltages: 3 kv (**Fig. 12a**); 0 kv (**Fig. 12b**). Bar = 400 nm.

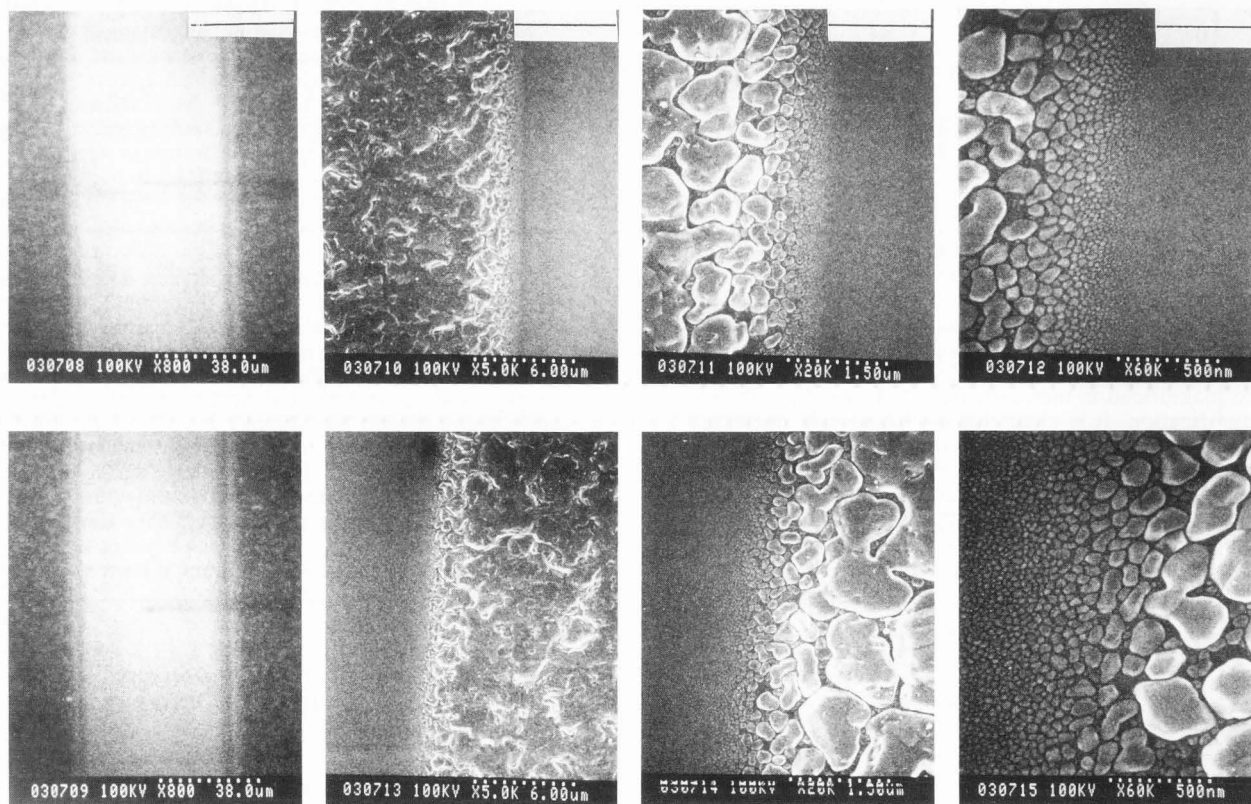


Figure 13. SEM micrographs of an Al film at the edge of the shadow zone formed by a wire mask on NCR HTO. The nominal film thickness is 270 nm. Substrate temperature: 300°C. Top row: Views of the left edge of the shadow zone. Bottom row: Views of the right edge of the same shadow zone. The dotted bars at the lower right hand corners of the micrographs are 30  $\mu$ m, 6  $\mu$ m, 1.5  $\mu$ m and 500 nm in length respectively for micrograph column pairs from left to right.

parameters derived from experimental measurements of diffusion distance and substrate temperature. This relationship reproduces the shape of the experimental curves and shows a maximum of diffusion distance near 200°C substrate temperature in agreement with experiment.

### Conclusions

Measurements have been made of Al atom diffusion distances which occur during physical vapor deposition (PVD), neutral cluster deposition (NCD), and ionized cluster beam deposition (ICB) on several types of substrate. For all deposition methods, and for all substrates, the maximum diffusion distance generally occurs at a substrate temperature near 200°C. The diffusion distances are found to be in the range of tens of micrometers.

### Acknowledgements

We thank Mr. Darryl Allman of NCR Microelectronics of Colorado Springs, Colorado for supplying the NCR HTO and LTO coated Si wafers, and also thank Mr. Ramzi Totari of Novellus Systems of San Jose, California for supplying the Novellus HTO, LTO, and nitride coated Si wafers.

### References

- Chopra KL. (1969). Thin Film Phenomena, McGraw-Hill, New York, p. 140-141.
- Dodson BW. (1987). Atomistic simulation of silicon beam deposition, Phys. Rev. **B36**, 1068-1074.
- Eyring H, Eyring EM. (1963). Modern Chemical Kinetics, Selected Topics in Modern Chemistry, Rhinhold, New York, p.6-7.
- Inoue M, Hashizume K, Tsuchikawa H. (1988). The properties of aluminum thin films sputter deposited at elevated temperatures, J. Vac. Sci. Technol. **A6**, 1636-1639.
- Levenson LL, Asano H, Tanaka T, Usui H, Yamada I, Takagi T. (1988). Al Surface Mobility on Si(111) during the initial stage of ICB deposition, J. Vac. Sci. Technol. **A6**, 1552-1556.
- Levenson LL, Usui H, Yamada I, Swartzlander AB. (1989). Anisotropic surface mobility of aluminum on Si(111) during the initial stage of vapor deposition, J. Vac. Sci. Technol. **A7**, 1206-1209.
- Levenson LL, Swartzlander AB, Usui H, Yamada I, Takagi T. (1989). Mat. Res. Soc. Proc. **128**, 131-136.
- Levenson LL, Swartzlander AB, Usui H, Yamada I. (1990). Aluminum surface mobility on two types of silicon oxide during ionized cluster beam deposition, Surf. and Interface Sci. **15**, 159-162.
- Levenson, LL, Swartzlander AB, Yahashi A, Usui H, Yamada I. (1990). Aluminum surface mobility on silicon nitride and on several silicon oxides, J. Vac. Sci. Technol. **A8**, 1147-1152.
- Phaneuf RJ, Williams ED. (1987). Surface phase separation of vicinal Si(111), Phys. Rev. Lett. **58**, 2563-2566.
- Takagi T. (1986). Ionized cluster beam technique for thin film deposition, Z. Phys. **D3**, 271-278.
- Venables, JA. (1986). Nucleation and growth processes in thin film formation, J. Vac. Sci. Technol. **B4**, 870-873.
- Venables JA, Droust T, Kariotis. (1987). Surface diffusion and nucleation processes in thin film formation: the case of Ag/Si (111), Mat. Res. Soc. Proc. **94**, 3-14.
- Yamamura Y, Yamada I. (1989). Computer studies of ionized Ag cluster beam deposition on amorphous carbon, Proc. 12th Symp. on Ion Sources and Ion-Assisted Technology, Tokyo, ed. by T. Takagi, published by Ion Beam Engineering Experimental Laboratory, Kyoto University, p.287-296.
- Zinke-Allmang M, Feldman LC. (1988). A novel technique to determine hetero-surface diffusion in semiconductor systems, Appl. Surf. Sci. **33/34**, 395-399.

### Discussion with Reviewers

**H.-J. Gossmann:** What is the spread of the patterned deposits due to the source geometry alone, i.e., in the complete absence of diffusion?

**Authors:** A 2 mm diameter nozzle source at a distance of 240 mm from the sample will produce a penumbra of 0.2  $\mu\text{m}$  and a 5.5 mm diameter orifice will produce a penumbra of 0.6  $\mu\text{m}$  when a 50  $\mu\text{m}$  diameter wire in contact with the substrate is used as a mask. In the UHV depositions, a 50  $\mu\text{m}$  wide slit placed 0.1 mm from the surface would give a penumbra of 0.8  $\mu\text{m}$ . Thus, in all cases, the spread of patterned deposits due to source geometry alone is expected to be less than 1  $\mu\text{m}$ .

**H.-J. Gossmann:** As pointed out by the authors, Dodson [Phys. Rev. B 36, 1068 (1987)] has calculated that 10 eV Si atoms in near-normal incidence on Si (111) come to rest within a few atomic distances from the point of impact. However, for glancing angles, Dodson obtains ranges of thousands of angstroms. It would be extremely interesting to check this prediction. Have experiments been done with off-normal incidence? If so, what are the results?

**Authors:** We have considered this type of experiment, but we have not attempted it.

**H.-J. Gossmann:** Eq. (1) assumes that re-evaporation is dominant, i.e., that  $\tau_s \ll t_d$ ,  $t_d = 1$  min being the deposition time. However, from Eq. (3) with  $v = 10^{12} \text{ s}^{-1}$  and with  $E_{\text{des}} \approx \Delta Q \approx 1.2 \text{ eV}$  one obtains  $\tau_s = 1.3 \times 10^4 \text{ s} \gg t_d$  at 80°C. Instead of making the above assumption, it would be better to solve the appropriate diffusion equation [for example see J.A. Venables, T. Droust and R. Kariotis, MRS Proc. 94, 3 (1987)] and extract  $Q_{\text{diff}}$  and  $Q_{\text{des}}$ . This would make this section much stronger and might also solve the puzzling result of the temperature dependent activation energies.

**Authors:** Eq. (1) does not imply that  $\tau_s \ll t_d$ .  $\tau_s$  is the mean time interval between impact and desorption.  $\tau_s$  is not related to  $t_d$ . However, if  $\tau_s \ll t_d$  does hold then no film is likely to be found after an attempted deposition! Therefore, even at a 400°C substrate temperature, it is important that  $\tau_s \gg t_d$  in these experiments. As for the approach of Venables, et. al., (Ref. 13 in the above paper), this requires an analysis of two experiments. One experiment involves an analysis of the nucleation parameters of the adsorbant on a well-defined substrate. The other experiment concerns an analysis of surface diffusion of the same adsorbant on the same substrate. The various energy parameters are then extracted on the basis of a model which requires consistency in the temperature dependencies and the pre-exponentials. The set of experiments carried out here contained only the diffusion set of experiments. Since at this time the nucleation experiments are lacking, we are unable to analyze our data in the same way as Venables et. al. On the other hand, it turns out that the "patch width" vs 1000/T curves measured by Venables et. al., (See Ref. 13)

can be modeled in the same way as Fig. 11 in this paper. This does not imply that the model is correct, only that it can parameterize similar diffusion data. Certainly, the approach taken by Venables et. al. is to be preferred.

H.-J. Gossmann: What are the error bars on distance and temperature measurements?

Authors: The error bars on (diffusion) distance are the sum of the maximum spread due to source geometry alone (1  $\mu\text{m}$ ) and the diameter of the primary electron beam (1  $\mu\text{m}$ ) used for Auger electron line scans. Thus the expected error is  $\pm 2 \mu\text{m}$ .

H.-J. Gossmann: Are the differences in diffusion distance with and without acceleration voltage, such as listed in Table 2, significant?

Authors: The general pattern in the data indicates that the ICB source (with or without ionization and acceleration) produces longer diffusion distances than simple effusion sources. Furthermore, at 200°C substrate temperatures, diffusion distances are generally larger for higher acceleration voltages. For some discussion of the influence of ion bombardment on surface diffusion, see Robinson, R.S. and Rossmagel, S.M., under Additional References.

M. Zinke-Allmang: The temperature dependence of  $\Delta Q$  has been attributed to a temperature dependence of  $Q_{\text{diff}}$ . Alternatively it might originate from a concentration dependence in Eq. (1): If Al clusters are present the spread of the deposited Al (6 nm per run) might be a process involving more than one time constant as shown in Eq. 2b of Zinke-Allmang and Feldman (see Additional References). If Al forms three-dimensional clusters then fewer but larger clusters are present at higher temperature due to cluster ripening. Thus the ratio of cluster sites and free adatom sites on the surface would vary with substrate temperature. The impact of this on the obtained diffusion length is not trivial since also desorption has to be considered.

Authors: Figures 12 and 13 in this paper illustrate some of the points raised by Dr. Zinke-Allmang. In Fig. 12, it is seen that an Al film nominally 6 nm thick forms three dimensional islands on the Si (111) surface. The shape of the islands depends on whether or not the Al beam is partially ionized and accelerated or neutral. Furthermore, at long diffusion distances (8.9  $\mu\text{m}$  in Fig. 12 a) under the mask, the influence of ionization and acceleration is lost and the shape of the islands resembles that of a neutral beam. Thus for an ionized and accelerated beam, the diffusion process in an area masked from impinging atoms and ions is somewhat different than the diffusion process in an area exposed to the beam. For thick films, the diffusion process at the edge of the masked area is even more complex because of a strong gradient in the size distribution of islands in the direction normal to the mask edge, as shown in Fig. 13. The dependence of the diffusion constant on surface coverage also has been discussed by Kobayashi et. al. (see Additional References).

Janice Reutt-Robey: Can interdiffusion by Al into the Si lattice be ruled out at higher temperatures? How will this affect the conclusions of this paper?

Authors: Diffusion coefficients and solid solubilities of Al in Si are given in Figs. 9.1.1 and 9.1.2 in the text by Tuck (see Additional References). At temperatures below 500°C, the diffusion coefficient is well below  $10^{-15} \text{ cm}^2 \text{ s}^{-1}$  and the solubility below  $1 \times 10^{19} \text{ cm}^{-3}$ . Lander and Morrison (see Additional References) have carefully studied the surface reactions of Al on Si (111) surfaces. Al forms a number of surface phases on Si (111). Long term annealing of Al films on Si (111) 700°C causes some solution of Al in Si. However, at temperatures below 500°C, no significant solution of Al in Si is expected.

#### Additional References

Kobayashi, Paik S. -M., Das Sarma, S. (1986). Kinetics and Energetics Studies at Surfaces and Interfaces, *J. Vac. Sci. Technol.* B4, 884-887.

Lander, J.J., Morrison, J. (1964). Surface Reactions of Silicon with Aluminum and with Indium, *Surface Science* 2, 553-565.

Robinson, R.S., Rossmagel, S.M. (1984). Diffusion processes in Bombardment-induced Surface Topography. In: Ion Bombardment Modification of Surfaces: Fundamentals and Applications. O. Auciello and R. Kelly, (Eds.). Elsevier Science Publishers, B.V. Amsterdam, p. 299-322.

Tuck, B. (1974). Introduction to Diffusion in Semiconductors, IEEE Monograph Series 16, Peter Peregrinus Ltd., Southgate House, Stevenage, Herfs., England, p. 224-227.

Zinke-Allmang, M., Feldman, L.C. (1988). Concentration Dependence of Surface Diffusion Coefficients in Clustering Systems, *Phys. Rev.* B37, 7010-7013.